Turbulent Mixing Model Based on Ordered Pairing

A. T. NORRIS and S. B. POPE

Sibley School of Mechanical and Aerospace Engineering, Cornell University, Ithaca, NY 14853

In Turbulent reactive flows the fluid composition at a point changes due to convection, reaction, and mixing (i.e., molecular transport). Modeling approaches based on the transport equation for the joint probability density function (jpdf) of velocity and composition have proved successful, largely because convection and reaction can be treated exactly, without modeling assumptions. Mixing has to be modeled, however, and current mixing models are deficient in several respects. The first contribution of this article is to define a model problem pertaining to turbulent diffusion flames in the flamelet regime. When applied to this problem, existing models incorrectly yield composition jpdfs corresponding to distributed combustion. The second contribution is to develop and demonstrate a new class of mixing models that performs satisfactorily for the model problem, and also for the case of the decaying field of a conserved scalar.

1. INTRODUCTION

The success of probability density function (pdf) methods [1] in the modeling of turbulent combustion is largely due to their ability to treat the nonlinear, coupled reactions between different chemical species. The complexity of the systems that are modeled varies from the simple, one-step irreversible, fast-chemistry problems considered by Dopazo and O'Brien [2], Janicka et al. [3], Nguyen and Pope [4], Pope and Anand [5] and Anand and Pope [6], to the multispecies, finite-rate systems employed by Pope [7], Pope and Correa [8], and Chen, et al. [9].

Although pdf methods offer several advantages over other methods, a weaknesses is the modelling of the mixing process.

The first mixing model, developed by Curl [10], had several defects, including an inability to develop a continuous pdf from a discontinuous initial distribution [11]. Modifications to Curl's model by Janicka et al. [12] overcame this defect, but problems concerning the shape of the predicted pdf remained.

For the turbulent mixing of a conserved passive scalar ξ, with pdf $\mathscr{P}_\xi(\zeta; t)$, the mean $\langle\xi\rangle$,

$$\langle\xi\rangle = \int_{-\infty}^{+\infty} \zeta \mathscr{P}_\xi(\zeta; t)\, d\zeta, \tag{1}$$

and the variance σ_ξ^2,

$$\sigma_\xi^2 = \int_{-\infty}^{+\infty} (\zeta - \langle\xi\rangle)^2 \mathscr{P}_\xi(\zeta; t)\, d\zeta, \tag{2}$$

can be used to define the standarized fluctuation,

$$\hat{\xi} = \frac{(\xi - \langle\xi\rangle)}{\sigma_\xi}. \tag{3}$$

The experimental evidence of Tavoularis and Corrsin [13], and the direct numerical simulations of turbulent mixing by Eswaran and Pope [14], show that asymptotically the pdf of $\hat{\xi}$, $\mathscr{P}_{\hat{\xi}}(\hat{\zeta})$, adopts the Gaussian distribution,

$$\mathscr{P}_{\hat{\xi}}(\hat{\zeta}) = \frac{1}{\sqrt{2\pi}} \exp\left(-\frac{\hat{\zeta}^2}{2}\right). \tag{4}$$

For the case of mixing in isotropic turbulence, it is found [11] that Curl's model (and its modifi-

Published by Elsevier Science Publishing Co., Inc.
655 Avenue of the Americas, New York, NY 10010

0010-2180/91/$3.50

cation [12]) yields asymptotic pdfs that differ greatly from the Gaussian density (Eq. 4). In particular the flatness factor $\langle \hat{\xi}^4 \rangle$ is infinite, rather than having the Gaussian value of 3. To address this problem a class of mixing models incorporating "age biasing" was developed by Pope [11] that yield asymptotic pdfs that are approximately Gaussian (e.g. flatness factors of 3.7). (In spite of the incorrect asymptotic pdf in isotropic turbulence, Curl's model (and its modifications) produce flatness factors of about 3 when applied to turbulent diffusion flames [4, 15].)

Preliminary application of these mixing models to hydrocarbon–air turbulent diffusion flames [16–19] revealed a separate defect reported by Pope et al. [20]. Subsequently Chen and colleagues [9, 15] have confirmed the problem encountered. Simply stated, the problem is that when applied to diffusion flames in the flamelet regime, current models can mix cold fuel with cold air to produce a cold, nonreactive, near-stoichiometric mixture. This is clearly physically incorrect (in the flamelet regime in the absence of local extinction).

In this article, a new class of mixing models is developed that substantially reduces the probability of nonreacting mixing of fuel and air in diffusion flames. First a test problem is developed that enables the performance of different mixing models in the flamelet region to be evaluated. This test problem is applied to the existing models, and their deficiencies are revealed and discussed. Then a new class of mixing models is described that offers improved performance over the existing models in the flamelet region. In order to improve the versatility of the new models, the scalar decay test used by Pope [11] is used to check on the shape of the asymptotic pdf of scalar fluctuations, and a compromise mixing scheme is proposed that performs well in both tests.

2. MODEL PROBLEM

In this section a model problem is constructed to test the performance of mixing models applied to turbulent non-premixed combustion in the flamelet regime. Bilger [21, 22] and Peters [23] provide reviews on the nature and theories of turbulent diffusion flames.

2.1. Combustion Regimes

To a first approximation, the qualitative nature of turbulent combustion is determined by the Damkohler number Da based on the Kolmogorov time scale τ_η,

$$\mathrm{Da} = \tau_\eta / \tau_c, \tag{5}$$

where τ_c is a characteristic reaction time [24]. For $\mathrm{Da} \ll 1$, there is distributed combustion: reaction has little effect on the microscale structure of the composition field, and current mixing models are satisfactory. For $\mathrm{Da} \gg 1$ there is flamelet combustion (but see Bilger [25]), and standard flamelet models [23] (or a flamelet model combined with a pdf method [26]) can be used. But for Da of order unity, the simple structure assumed in flamelet models breaks down. This is a regime of much current interest [9, 16–19], and our aim is to extend the validity of mixing models to it. In this context, therefore, a severe test of mixing models is to apply them in the flamelet regime ($\mathrm{Da} \gg 1$).

2.2. Thermochemistry

We consider the simplest possible thermochemistry. Fuel and oxidant react rapidly in a one-step irreversible reaction to form the product. The mass fraction of the three species are denoted by $Y_F(\mathbf{x}, t)$, $Y_O(\mathbf{x}, t)$ and $Y_P(\mathbf{x}, t)$. In the limit of infinite Da (and with other standard assumptions) these mass fractions are uniquely related to the mixture fraction $\xi(\mathbf{x}, t)$ by, for example,

$$Y_P(\mathbf{x}, t) = Y_P^f(\xi(\mathbf{x}, t)), \tag{6}$$

where the superscript f stands for "fully burned," and the functions Y_P^f, Y_F^f, and Y_O^f are sketched in Fig. 1.

The well-established [24] picture of turbulent nonpremixed combustion with this thermochemistry and $\mathrm{Da} \gg 1$ is that reaction is confined to the stoichiometric surface defined by $\xi(\mathbf{x}, t) = \xi_s$. Fuel and oxidant diffuse toward this reaction

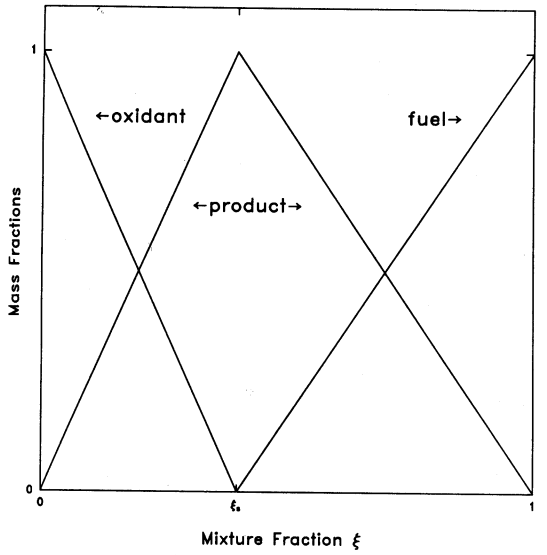

Fig. 1. Schwab-Zeldovich functions $Y_F^f(\xi)$, (fuel), $Y_O^f(\xi)$, (oxidant), and $Y_P^f(\xi)$, (products).

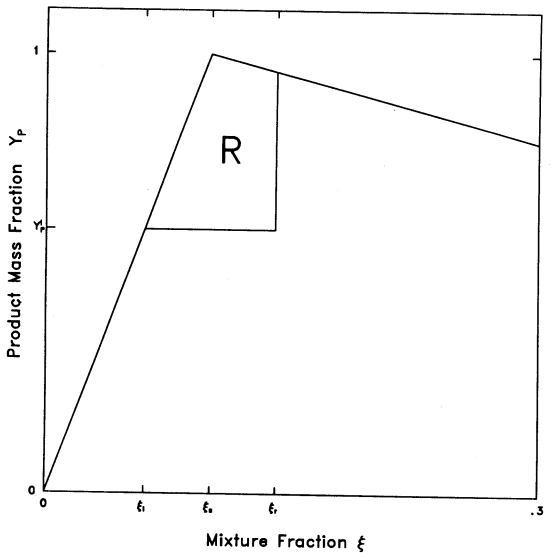

Fig. 2. Sketch showing the rich (ξ_r) and the lean (ξ_l) limits of the reaction zone R, which is bounded from below by Y_P^l.

sheet from opposite sides, and are there completely converted to product. Consequently fuel and oxidant never coexist.

In general (for finite or infinite Da) we define $S(\xi, Y_P)$ to be the creation rate of Y_P due to chemical reaction. Note that $S(\xi, Y_P)$ is defined for $0 \leq Y_P \leq Y_P^f(\xi)$, and that $S(\xi, Y_P^f(\xi))$ is zero. For the infinite Da flame-sheet limit to exist, it is sufficient for $S(\xi, Y_P)$ to be infinite in an arbitrarily small region of the $\xi - Y_P$ plane at $(\xi_s, Y_P^f(\xi_s))$. However, such a small region imposes an unnecessarily severe test on the mixing model. Instead we specify S to be infinite in the region R shown on Fig. 2. The stoichiometric mixture fraction $\xi_s = 0.05$, and the lean and rich limits of the reaction zone $\xi_l = 0.03$, $\xi_r = 0.07$, are chosen to correspond, approximately, to hydrogen–air or methane–air flames [25]. The lower limit of the reactive region R is chosen, somewhat arbitrarily, to be $Y_P^l = 0.6$.

This thermochemical model was originally proposed by Pope et al. [20]; a similar model has been used by Chen and Kollmann [15].

(Referring to Fig. 2, as the boundary of the reaction zone is crossed, the reaction rate S jumps discontinuously from zero to infinity. It may be preferred to regard S as increasing continuously to a large but finite value in a very small interval. Then the resulting fields $\xi(\mathbf{x}, t)$, $Y_P(\mathbf{x}, t)$ are smoother and possible technical difficulties are avoided.)

2.3. Flow Specification

The thermochemical model presented in the previous section can be applied to any turbulent nonpremixed flow. For simplicity, however, we consider constant-density, statistically stationary, homogeneous isotropic turbulence with zero mean velocity. The turbulent kinetic energy and its dissipation rate are taken to be unity.

The thermochemical variables $\xi(\mathbf{x}, t)$ and $Y_P(\mathbf{x}, t)$ are statistically homogeneous. We introduce ζ and y as sample-space variables corresponding to ξ and Y_P. Thus, the joint pdf of ξ and Y_P (i.e., the probability density of $\xi(\mathbf{x}, t) = \zeta$, $Y_P(\mathbf{x}, t) = y$) is $\mathscr{P}_{\xi Y_P}(\zeta, y; t)$ (independent of $\mathbf{x}$). Initially ($t = 0$), the composition field is specified to correspond to flamelet combustion [i.e., $Y_P(\mathbf{x}, 0) = Y_P^f(\xi(\mathbf{x}, 0))$], implying

$$\mathscr{P}_{\xi Y_P}(\zeta, y; 0) = \mathscr{P}_{\xi}(\zeta; 0)\delta(y - Y_P^f(\zeta)). \tag{7}$$

The initial pdf of ξ, $\mathscr{P}_\xi$, is specified to be a β-function distribution with a mean $\langle\xi\rangle = 0.1$ and variance 0.01. These values are obtained from the experimental work of Masri et al. [17] in a piloted methane–air flame and can be considered typical of hydrocarbon–air flames.

2.4. Correct Behavior

Applied to the test problem, an ideal mixing model has the following behavior:

1. The mean $\langle\xi\rangle$ is constant.
2. The variance of ξ decreases with time.
3. The product Y_P is confined to the fully burned line $Y_P^f(\xi)$.
4. Asymptotically (for large t) the pdf of ξ decays as a Gaussian (as suggested by experimental and numerical evidence [13, 14]).

There is no difficulty in constructing models that satisfy conditions (1) and (2) exactly. We are not concerned here with the rate of decay of the variance: rather we concentrate on the shape adopted by the joint pdf.

The third condition implies that the joint pdf is

$$\mathscr{P}_{\xi Y_P}(\zeta, y; t) = \mathscr{P}_\xi(\zeta; t)\delta(y - Y_P^f(\zeta)), \quad (8)$$

and also

$$\langle Y_P \mid \xi = \zeta\rangle = Y_P^f(\zeta), \quad (9)$$

that is, the mean of Y_P, conditional on ξ is $Y_P^f(\zeta)$.

The requirement that the asymptotic pdf of ξ is Gaussian is evaluated by calculating the evolution with time of the moments of ξ

$$\mu_n(t) = \frac{1}{\sigma_\xi^n}\int_{-\infty}^{+\infty}(\zeta - \langle\xi\rangle)^n \mathscr{P}_\xi(\zeta)\, d\zeta, \quad (10)$$

where σ_ξ is the standard deviation of ξ evaluated at time t. In order for the distribution to decay to a Gaussian, the odd moments $n = 3, 5, \ldots$ are required to decay to zero, while the even moments asymptote to their Gaussian values of 3 for $n = 4$, 15 for $n = 6$, etc. Whether the moments reach an asymptotic value, and how close they are to the Gaussian quantities, is a measure of how well the mixing model performs with respect to condition 4. (This condition is a form of the scalar decay test used by Pope [11], but with a different initial distribution of the scalar.)

3. EXISTING MODELS

The first stochastic mixing model was proposed by Curl [10] in 1963 and has formed the basis of many subsequent schemes, such as those by Janicka et al. [12] and Pope [11]. In this section, the mixing mechanism of Curl's model and the Modified Curl's model developed by Janicka et al. are described in the context of the diffusion flame test developed in Sec. 2. These two models are found to perform poorly in the diffusion flame test and the reasons for the deficient performance are discussed and possible methods of improving the models proposed.

3.1. Mixing Mechanism

At time $t = 0$, the initial jpdf of ξ and Y_P, $\mathscr{P}_{\xi Y_P}(\zeta, y; 0)$ (Eq. 7) is approximated by a discrete distribution of N Dirac delta functions,

$$\mathscr{P}_{\xi Y_P}(\zeta, y; 0) \approx \frac{1}{N}\sum_{i=1}^{N}\delta(\zeta - \xi_i)\delta(y - Y_P^f(\xi_i)). \quad (11)$$

The error in the discrete approximation of $\mathscr{P}_{\xi Y_P}(\zeta, y; 0)$ (Eq. 11) is inversely proportional to $\sqrt{N}$, [1]; thus for accuracy the value of N should tend to infinity. However, an increase in the value of N results in a corresponding increase in the number of calculations that must be performed in implementing the model. A compromise must therefore be struck between an acceptable level of accuracy in the discrete approximation, and the computational resources available. (For all calculations described in this article, the value of $N = 2^{15} = 32,768$ is used.)

Each Dirac delta function in the approximation of $\mathscr{P}_{\xi Y_P}(\zeta, y; 0)$ (Eq. 11) can be considered as a stochastic particle with a mixture fraction of ξ_i and product mass fraction of Y_{Pi}. The evolution

of the joint pdf $\mathscr{P}_{\xi Y_P}(\zeta, y; t)$ with time is achieved by the interaction and movement of these stochastic particles in (ξ, Y_P) space by the mechanism described below.

During a small time interval δt, two particles i and j with properties (ξ_i, Y_{Pi}) and (ξ_j, Y_{Pj}) are selected, by choosing i and j at random from (1, N), without replacement. The values of these two particles are then changed by the mixing scheme to (ξ_i^*, Y_{Pi}^*) and (ξ_j^*, Y_{Pj}^*), and the two particles, with their new values are substituted back into the ensemble. The process then repeats for the next time interval.

The time interval δt governs the rate at which the joint pdf evolves and is calculated from

$$\delta t = 1/\beta\omega N, \tag{12}$$

where ω is the rate at which the standard deviation of ξ decays and β is a constant, determined by the mechanism of mixing [1, 11].

The new values of the two particles i and j are given by

$$\begin{aligned}(\xi_i^*, Y_{Pi}^*) &= (1-\alpha)(\xi_i, Y_{Pi}) \\ &\quad + \frac{\alpha}{2}((\xi_i, Y_{Pi}) + (\xi_j, Y_{Pj})), \\ (\xi_j^*, Y_{Pj}^*) &= (1-\alpha)(\xi_j, Y_{Pj}) \\ &\quad + \frac{\alpha}{2}((\xi_i, Y_{Pi}) + (\xi_j, Y_{Pj})).\end{aligned} \tag{13}$$

For Curl's model, $\alpha = 1$, which gives the new values of the two particles as the midpoint between the particles i and j in (ξ, Y_P) space. For the Modified Curl's model, α is a random variable, $0 \le \alpha \le 1$ with distribution $A(a)$. In order to minimize the occurrence of particles mixing across R without reaction taking place, $A(\alpha)$ is chosen as a uniform distribution between zero and 0.05.

Should the new value of a particles lie within the reaction zone R, then due to reaction that particle is raised up to the fully burned line, i.e., Y_{pi}^* is replaced by $Y_P^f(\xi_i)$, and/or Y_{Pj}^* is replaced by $Y_P^f(\xi_j)$. (A similar form of "Reaction Zone Conditioning" has been used by Chen and Kollmann [15], but with finite reaction rates.)

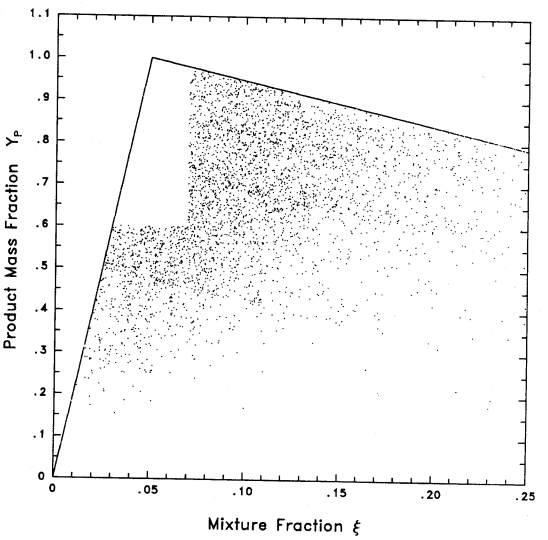

Fig. 3. Scatter plot of particle position at time $t = 0.4$, produced by the diffusion flame test with Curl's mixing model. (For clarity, only 8096 out of 32 768 particle positions are shown.)

3.2. Curl's Model

For Curl's model (with a decay rate $\omega = 1$ and $\beta = 4.0$) a scatter plot of particle position after an elapsed time of $t = 0.4$ (Fig. 3) shows that a significant number of particles have moved away from the fully burned line. This joint pdf suggests that distributed combustion (Da $\ll 1$) is occurring, rather than the prescribed flamelet combustion. The evolution of the quantity $\langle Y_P \mid \xi \rangle$ is shown in Fig. 4, which shows the drift of expected particle position away from the fully burned line, indicating that the deviation from the correct position is not a transient effect. The evolution of the normalised moments of ξ is shown in Fig. 5. The mean is seen to remain constant, and the variance decays exponentially to zero—the correct results. However, the higher order moments do not exhibit Gaussian behavior. The odd moments μ_3 and μ_5 do not decay toward zero, indicating that the distribution is not asymptoting toward a symmetric pdf. The even moments μ_4 and μ_6 do not asymptote to their respective Gaussian values of 3 and 15, but rather show a steady increase (and also an increase in their statistical error) as time progresses.

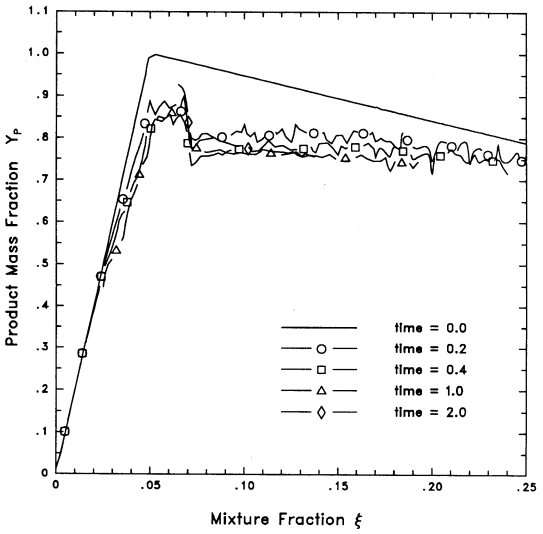

Fig. 4. Evolution of $\langle Y_P \mid \xi \rangle$ with time, produced by the diffusion flame test with Curl's mixing model.

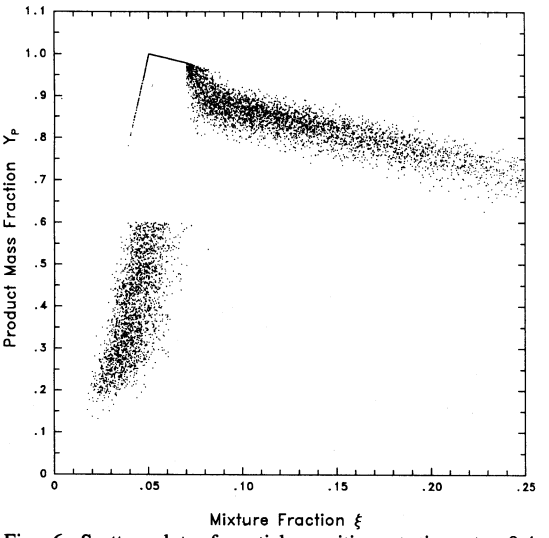

Fig. 6. Scatter plot of particle position at time $t = 0.4$, produced by the diffusion flame test with the Modified Curl's mixing model. (For clarity, only 8096 out of 32 768 particle positions are shown.)

3.3. Modified Curl's Model

The performance of the Modified Curl's model ($\omega = 1$ and $\beta = 82.8$) in the diffusion flame test is similar to that of Curl's model, despite the difference in the selection of α. The scatter plot at time $t = 0.4$ (Fig. 6) shows an improvement over Curl's model (Fig. 3), with the particle positions lying in a band, close to $Y_P^f(\xi)$. However, the evolution of $\langle Y_P \mid \xi \rangle$ (Fig. 7) shows an increasing departure of the expected particle position from $Y_P^f(\xi)$ with time, suggesting that the

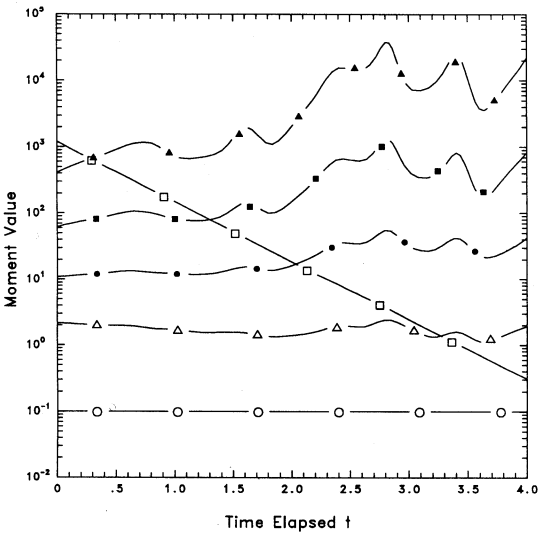

Fig. 5. Evolution of the moments μ_n of ξ produced by the diffusion flame test with Curl's mixing model. ○, mean; □, variance × 10^5; △, skewness; ●, flatness; ■, fifthness; ▲, superskewness.

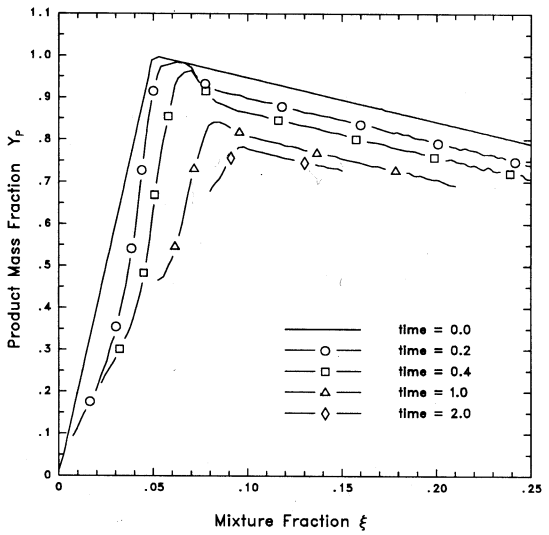

Fig. 7. Evolution of $\langle Y_P \mid \xi \rangle$ with time, produced by the diffusion flame test with the Modified Curl's mixing model.

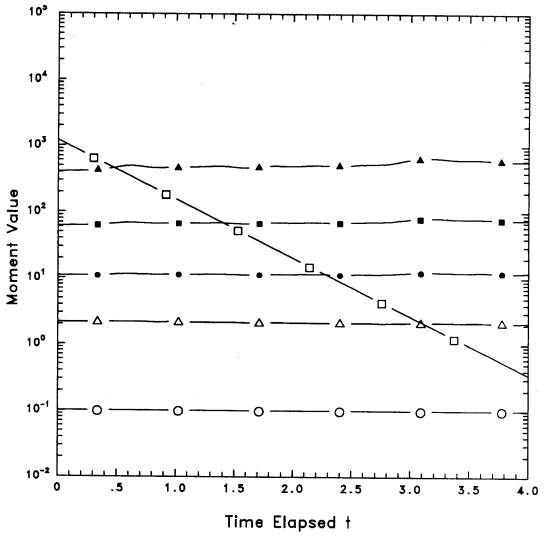

Fig. 8. Evolution of the moments μ_n of ξ produced by the diffusion flame test with the Modified Curl's mixing model. ○, mean; □, variance × 10^5; △, skewness; ●, flatness; ■, fifthness; ▲, superskewness.

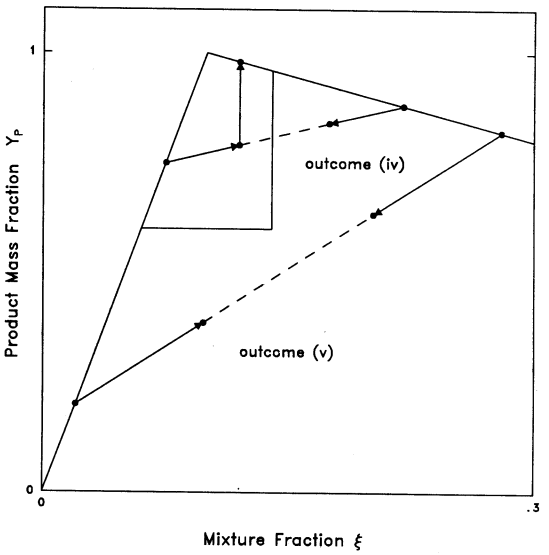

Fig. 9. Mixing outcomes (4) and (5) that result in particles being moved away from $Y_P^f(\xi)$.

Modified Curl's model will yield results less and less representative of high Da reaction as time progresses. The evolution of the normalized moments of ξ (Fig. 8) shows the same trends as observed for Curl's model: the mean and variance behaving correctly while the higher moments show no evidence of relaxing to Gaussian values. Chen and Kollmann [6] have produced somewhat similar results to those shown in Fig. 6 with the Modified Curl's mixing model, though with different reaction zone size and reaction rate.

3.4. Discussion

The performance of the two models in the diffusion flame test shows that they are unable to produce the correct joint pdf of ξ and Y_P for a high Da flame, and that the pdf of the conserved scalar ξ does not asymptote to a Gaussain distribution. For the present, we address only the former defect.

The less-than-satisfactory jpdf obtained for these two models can be explained by the mixing process. Starting with a pair of particles residing on the fully burned line, there are five possible outcomes of the mixing process:

1. Both mixed particles stay on $Y_P^f(\xi)$ because $\xi_i > \xi_s$ and $\xi_j > \xi_s$.
2. Both mixed particles stay on $Y_P^f(\xi)$ because $\xi_i < \xi_s$ and $\xi_j < \xi_s$.
3. The two particles are removed from $Y_P^f(\xi)$ by mixing, but the final particle values are both in R, and so both particles return to $Y_P^f(\xi)$ due to reaction.
4. The two particles are removed from $Y_P^f(\xi)$ by mixing; one of the final particle values is in R, and so that particle returns to $Y_P^f(\xi)$, while the other remains in a non-fully burned state.
5. The two particles are removed from $Y_P^f(\xi)$ by mixing; neither of the final particle values is in R, and so both particles remain in a non-fully burned state.

Clearly the last two mixing outcomes—sketched in Fig. 9—are the mechanism responsible for the drift of the jpdf away from $Y_P^f(\xi)$. Both outsomes (4) and (5) are characterized by the selection of pairs of particles with values of ξ that lie on either side of ξ_s, and whose difference is large compared to the width of the reaction zone R,

i.e.,

$$(\xi_s - \xi_a)(\xi_s - \xi_b) < 0$$

$$|\xi_a - \xi_b| \gg \xi_r - \xi_l. \tag{14}$$

Thus for a mixing scheme to perform well in the diffusion flame test, the selection of particle pairs must be biased against selecting partners with the two properties described above.

4. ORDERED PAIRING MODEL

In this section, a new class of mixing models is developed based on the technique of ordered selection of particle pairs. These models are shown to give superior performance over existing models in the diffusion flame test, as well as providing an asymptotic pdf of ξ with finite normalized moments.

4.1. Motivation

In the previous section it was shown that the drift of $\mathscr{P}_{\xi Y_P}(\zeta, y)$ away from the fully burned line $Y_P^f(\zeta)$ is caused by the selection of pairs of particles that possess the properties given in Eq. 14. In existing models mixing occurs between particles with a mixture fraction difference of order one standard deviation of ξ, σ_ξ. Clearly, if the selection of particle pairs is biased to ensure that the partners have similar values of ξ, i.e., $|\xi_a - \xi_b| \ll \sigma_\xi$, then the incidence of mixing across ξ_s is reduced, giving a closer fit to the desired jpdf [20].

This requirement also appeals to the physical aspects of mixing. The equation governing mixing is

$$\frac{D\xi}{Dt} = \Gamma \nabla^2 \xi, \tag{15}$$

where Γ is the molecular diffusivity. This shows that $\xi(\mathbf{x})$ is affected by the ξ field within an infinitesimal neighborhood of $\mathbf{x}$, where ξ differs infinitesimally from $\xi(\mathbf{x})$.

In order to achieve this selection bias, the technique of ordered selection is introduced.

4.2. Ordered Pairing Scheme

During a small time interval δt, (Eq. 12), a group of n particles with indices $\pi_1, \pi_2, \ldots, \pi_n$, and properties $(\xi_{\pi_1}, Y_{P\pi_1}), (\xi_{\pi_2}, Y_{P\pi_2}), \ldots, (\xi_{\pi n}, Y_P\pi_n)$, are selected without replacement from the ensemble of N stochastic particles. The value of n is governed by the requirement that it should be even to allow the particles to be paired with each other, with no unpaired particle left. We also require that $4 \leq n \ll N$, where the upper limit is to limit the chances of selecting the same group of particles in the next time step. Four is chosen as the lower limit, since with $n = 2$ the existing models are recovered. Throughout this paper a value of $n = 8$ is used. We now define a reordering, $\rho_1, \rho_2, \ldots, \rho_n$, of the indices of the n particles so that

$$\xi_{\rho 1} \leq \xi_{\rho 2} \leq \cdots \leq \xi_{\rho n} \tag{16}$$

These particles are known as a group of order particles.

The pairing of the order particles is accomplished by the use of a selection matrix S_{ij}. The elements of S_{ij} are composed of ones and zeros, a one signifying that the ith order particle is to be paired with the jth order particle, and a zero represents no pairing between the ith and jth order particles. There are m of these selection matrices, $S_{ij}^{(k)}$ $(k = 1, 2, \ldots, m)$, with P_k being the probability of $S_{ij}^{(k)}$. The expectation of S_{ij} is P_{ij}, the mixing matrix, i.e.,

$$P_{ij} = \langle S_{ij} \rangle = \sum_{k=1}^{m} P_k S_{ij}^{(k)}. \tag{17}$$

The elements of P_{ij} give the probability that the ith order particle has the jth order particle as its partner. The order particle pairs are now mixed by the same means as the Modified Curl's model (Eq. 13), with the same distribution of α, and the new values substituted back into the ensemble.

Certain restrictions on the selections of the elements of $S_{ij}^{(k)}$ (and thus P_{ij}) can be developed in response to certain assumptions made about the mixing model. First we disallow self-selection, and consequently the diagonal elements of $S_{ij}^{(k)}$

and hence P_{ij} are all zero. In addition we require that the expectation of ξ does not change with time. This is accomplished by the selection of $S_{ij}^{(k)}$ such that the sums of the columns equal one, i.e.,

$$\sum_{i=1}^{n} P_{ij} = 1. \tag{18}$$

For this condition to be satisfied, it is sufficient that $S_{ij} = S_{ji}$ (see Appendix A). (A physical interpretation of this condition is that no two or more order particles may select the same partner at the same time.)

By suitable choice of P_{ij} it is possible to recover the existing models. In order to negate the effects of ordering, the requirement is that each order particle should have equal likelihood of selecting any other order particle as its partner. This results in

$$P_{ij} = \begin{cases} 1/(n-1), & i \neq j, \\ 0, & i = j, \end{cases} \tag{19}$$

which recovers the Modified Curl's model. By selecting α in Eq. 13 equal to unity, Curl's model is recovered.

4.3. Adjacent Pairing

The requirement that the difference in the value of ξ between particle pairs be minimized is best met by the selection of adjacent order particles as partners, i.e., particle ρ_1 pairs with particle ρ_2, particle ρ_3 pairs with particle ρ_4, etc. This is achieved through the choices $m = 1$, $P_1 = 1$, and

$$S_{ij}^{(1)} = P_{ij} = \begin{Bmatrix} 0 & 1 & 0 & 0 & 0 & 0 & 0 & 0 \\ 1 & 0 & 0 & 0 & 0 & 0 & 0 & 0 \\ 0 & 0 & 0 & 1 & 0 & 0 & 0 & 0 \\ 0 & 0 & 1 & 0 & 0 & 0 & 0 & 0 \\ 0 & 0 & 0 & 0 & 0 & 1 & 0 & 0 \\ 0 & 0 & 0 & 0 & 1 & 0 & 0 & 0 \\ 0 & 0 & 0 & 0 & 0 & 0 & 0 & 1 \\ 0 & 0 & 0 & 0 & 0 & 0 & 1 & 0 \end{Bmatrix}. \tag{20}$$

The performance of this mixing model ($\omega = 1$ and $\beta = 620.0$) in the diffusion flame test is now discussed.

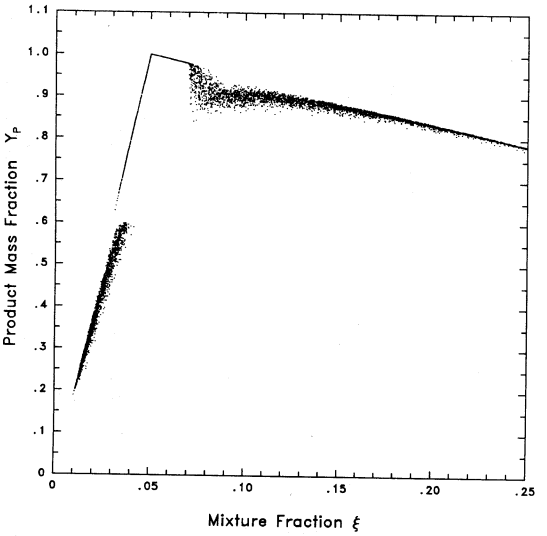

Fig. 10. Scatter plot of particle position at time $t = 0.4$, produced by the diffusion flame test with the Adjacent Pairing Scheme. (For clarity, only 8096 out of 32 768 particle positions are shown.)

The scatter plot of particle position in (ξ, Y_P) space at time $t = 0.4$ is shown in Fig. 10. The clustering of particles about $Y_P^f(\xi)$ shows that this mixing model closely predicts the occurrence of high Da or flamelet combustion, as opposed to the incorrect predictions of the existing models (Figs. 3 and 6). This result is reinforced by Fig. 11, which shows the evolution of $\langle Y_P \mid \xi \rangle$. The deviations of expected particle position from Y_P^f are seen to reach a maximum by time $t = 0.4$ and then become smaller, the value at time $t = 2.0$ being positioned almost on Y_P^f. The evolution of the normalized moments of ξ are shown in Fig. 12. The mean and variance evolve in the same manner as existing models; however, the odd higher-order moments ($n = 3, 5$) decay exponentially to zero, indicating that the pdf of ξ asymptotes to a symmetric distribution. Also the higher-order even moments ($n = 4, 6$) asymptote toward constant values of 1.5 and 2.9, respectively, suggesting that a stationary pdf of ξ has been achieved. However, these values of flatness and superskewness are much lower than the Gaussian values of 3.0 and 15.0, which suggests

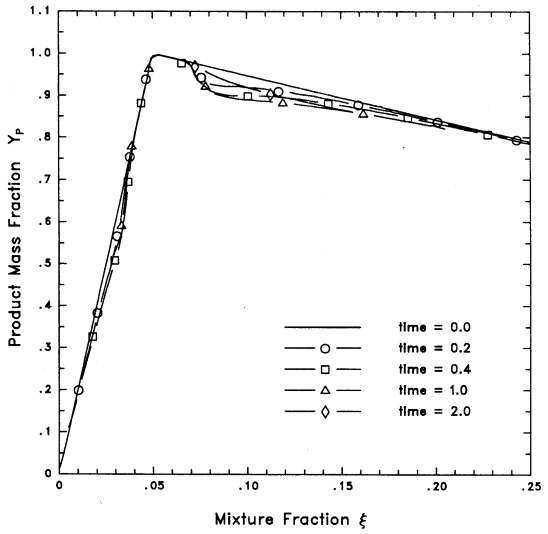

Fig. 11. Evolution of $\langle Y_P \mid \xi \rangle$ with time, produced by the diffusion flame test with the Adjacent Pairing Scheme.

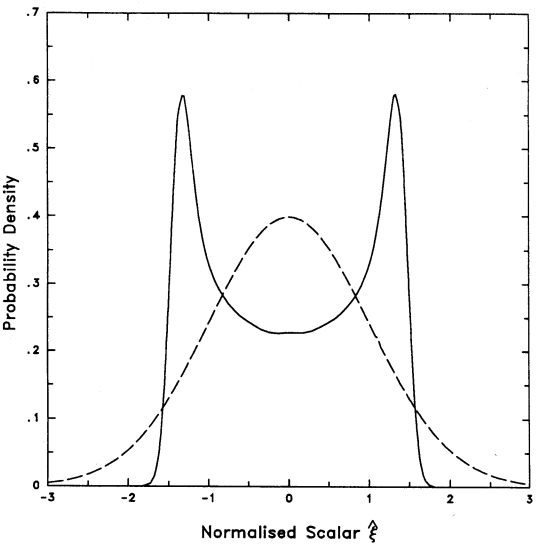

Fig. 13. Asymptotic pdf of ξ produced by the Scalar Decay Test, using the Adjacent Pairing Scheme. Gaussian distribution shown by dashed line.

that the stationary pdf has significantly smaller tails than a Gaussian.

The adjacent pairing scheme's performance in the scalar decay test [11] is now evaluated. This test takes an initial pdf of a scalar ξ, $\mathscr{P}_\xi(\zeta)$, with a distribution composed of two delta functions of equal size at $\xi = \pm 1$. The mixing model is then used to predict the evolution of $\mathscr{P}_\xi(\zeta)$ with time. Experimental evidence shows that the pdf should asymptote to a Gaussian; thus the performance of the mixing model is judged by how close the asymptotic pdf of ξ comes to a Gaussian. The shape of the asymptotic pdf produced by the adjacent pairing scheme in this test is shown in Fig. 13. Clearly this model produces a very poor representation of a Gaussian.

Thus the adjacent pairing scheme gives excellent results in the diffusion flame test, and although the pdf of ξ does not decay to a Gaussian, a symmetric pdf with finite moments is achieved.

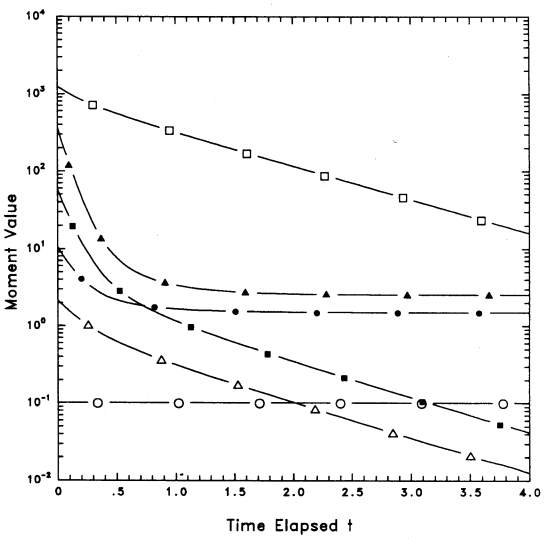

Fig. 12. Evolution of the moments μ_n of ξ produced by the diffusion flame test with the Adjacent Pairing Scheme. ○, mean; □, variance × 10^5; △, skewness; ●, flatness; ■, fifthness; ▲, superskewness.

4.4. Compromise Pairing

In the previous section it was shown that the adjacent pairing scheme gives excellent performance in yielding the correct jpdf in the diffusion flame test. However, the asymptotic pdf of ξ is far from Gaussian. In order to improve the versatility of the mixing scheme, a compromise pairing scheme is suggested, which performs well in the diffusion flame test, but also gives a pdf of ξ that is closer to Gaussian. In order to assist in the selection of a new particle pairing scheme, a

Gaussian decay test is developed (see Appendix B). This test evaluates the change of an initially Gaussian pdf of a scalar ξ, $\mathscr{P}_\xi(\zeta)$, due to the influence of the particle pairing scheme. This change is illustrated by the plotting of the function $Q(\zeta)$, defined in Appendix B, against the sample space variable ζ. For Gaussian decay, the plot is a straight line of gradient -1 passing through the origin. Any deviation from this line indicates that the pdf does not evolve as a Gaussian. For the case of adjacent pairing described in the previous section, the plot of ζ against $Q(\zeta)$ is shown in Fig. 14. The deviation from the correct result is most severe at the origin, where a positive gradient is present, while at $\zeta = \pm 3$ the plot has a gradient of -1. The pdf of ξ shown in Fig. 13 confirms the non-Gaussian result.

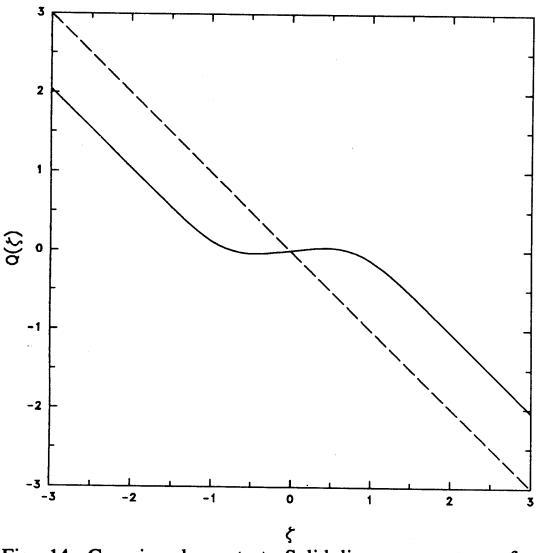

Fig. 14. Gaussian decay test. Solid line represents performance of the Adjacent Pairing Scheme; dashed line represents Gaussian decay.

By trying different combinations of order-particle pairing, a compromise pairing scheme has been developed, with P_{ij} given by

$$P_{ij} = \frac{1}{20}\begin{Bmatrix} 0 & 12 & 8 & 0 & 0 & 0 & 0 & 0 \\ 12 & 0 & 0 & 0 & 8 & 0 & 0 & 0 \\ 8 & 0 & 0 & 6 & 3 & 3 & 0 & 0 \\ 0 & 0 & 6 & 0 & 3 & 3 & 8 & 0 \\ 0 & 8 & 3 & 3 & 0 & 6 & 0 & 0 \\ 0 & 0 & 3 & 3 & 6 & 0 & 0 & 8 \\ 0 & 0 & 0 & 8 & 0 & 0 & 0 & 12 \\ 0 & 0 & 0 & 0 & 0 & 8 & 12 & 0 \end{Bmatrix} \tag{21}$$

The Gaussian decay test gives the plot of ζ against $Q(\zeta)$ shown in Fig. 15. This shows a closer fit to the straight line than for the adjacent pairing scheme, and the gradient of the plot is positive everywhere, indicating that the pdf of ξ can be expected to be closer to Gaussian than the adjacent pairing scheme.

Applying the compromise scheme ($\omega = 1$ and $\beta = 215.2$) to the diffusion flame test reveals a slightly inferior result to that of the adjacent pairing scheme. The scatter plot of particle position (Fig. 16) shows a larger spread of values away from the fully burned line than in Fig. 10. This deviation is a result of the pairing of nonadjacent order particles; thus raising the expected difference of ξ between particle pairs compared to the adjacent pairing scheme. This result, however, is still superior to that of the existing schemes shown in Figs. 3 and 6 in that the particles are still concentrated near $Y_P^j(\xi)$. The evolution of the expected conditional particle position $\langle Y_P \mid \xi \rangle$ (Fig. 17) shows a small deviation

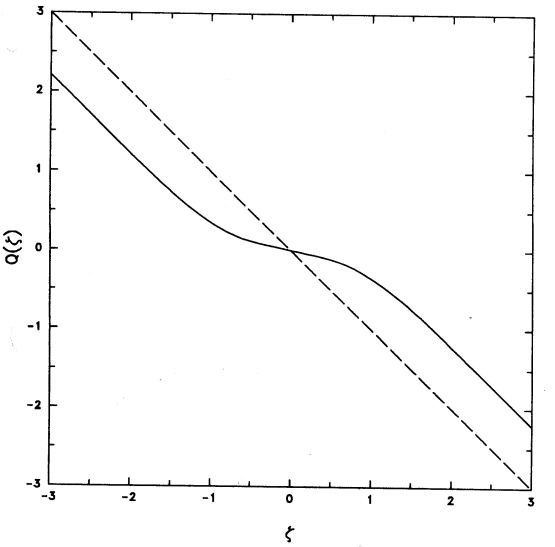

Fig. 15. Gaussian decay test. Solid line represents performance of the Compromise Pairing Scheme; dashed line represents Gaussian decay.

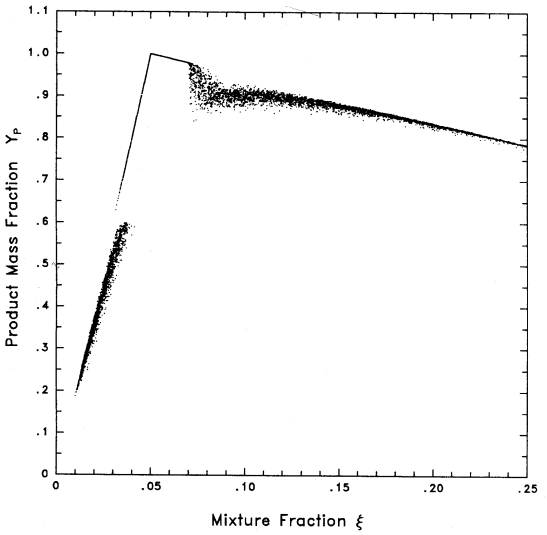

Fig. 16. Scatter plot of particle position at time $t = 0.4$, produced by the diffusion flame test with the Compromise Pairing Scheme. (For clarity, only 8096 out of 32 768 particle positions are shown.)

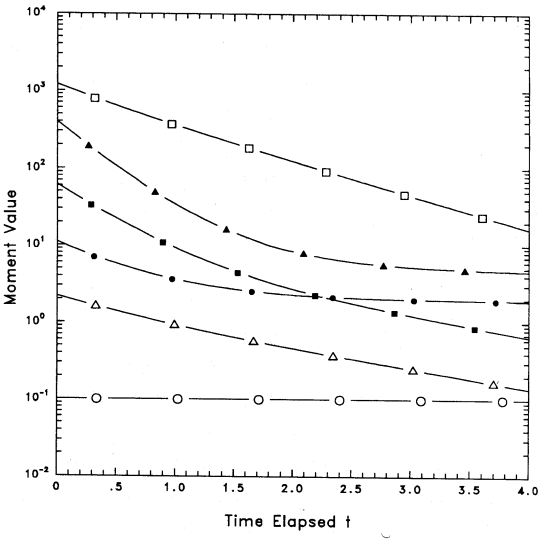

Fig. 18. Evolution of the moments μ_n of ξ produced by the diffusion flame test with the Compromise Pairing Scheme. ○, mean; □, variance × 10^5; △, skewness; ●, flatness; ■, fifthness; ▲, superskewness.

from $Y_P^f(\xi)$; however, as in the adjacent pairing scheme the value of $\langle Y_P \mid \xi \rangle$ at time $t = 2.0$ has moved back toward the fully burned line.

The evolution of the normalized moments of ξ, shown in Fig. 18, demonstrates the same trends as those of the adjacent pairing scheme. The only significant difference is in the asymptotic values of the flatness and superskewness ($n = 4$, 6), which have values of 2.1 and 6.5, respectively. These are closer to the Gaussian values of 3.0 and 15.0 than those of the adjacent pairing scheme.

The performance of the model in the scalar decay test reflects this improvement. Figure 19 shows the asymptotic pdf produced by this test, and, although non-Gaussian, it does not display the bimodal shape exhibited by Fig. 13.

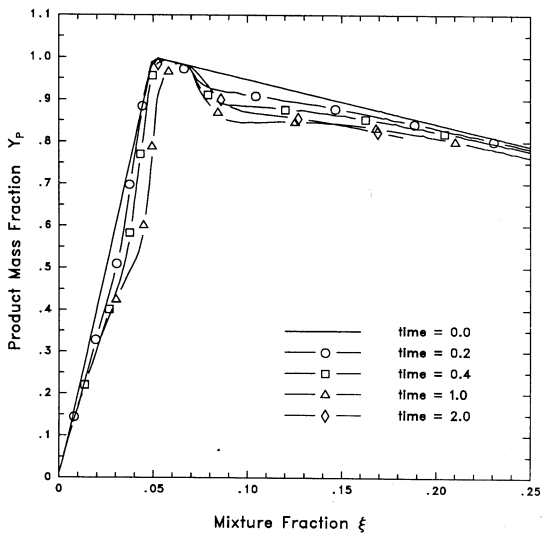

Fig. 17. Evolution of $\langle Y_P \mid \xi \rangle$ with time, produced by the diffusion flame test with the Compromise Pairing Scheme.

5. DISCUSSION

In the previous section two examples of the ordered pairing class of mixing models were described and tested. We now offer some comments on the class of models that has been developed.

This class of model is restricted in application to problems in which there is an unambiguously defined scalar ξ. This requirement is to ensure that the linearity and independence principles [27] are not violated.

Ther performance of these models in the diffusion flame test is improved by the selection of a high value of n, as this lowers the expected difference in ξ between particle pairs. However,

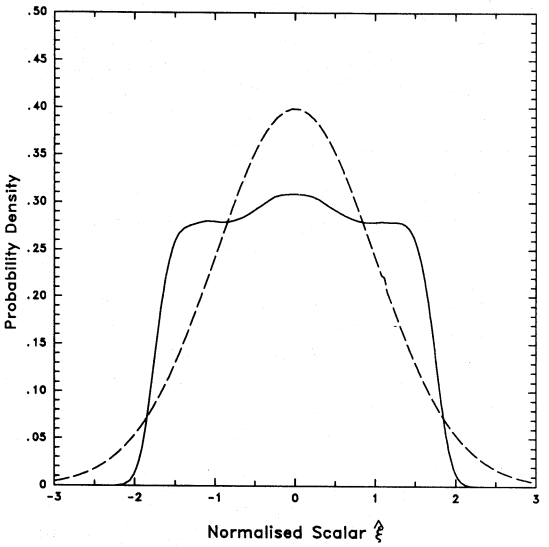

Fig. 19. Asymptotic pdf of ξ produced by the Scalar Decay Test, using the Compromise Pairing Scheme. Gaussian distribution shown by dashed line.

the increase in computer time required to order and mix the increased number of order particles is a reason against the selection of an overly large value of n. The choice of small values of n should also be avoided, as the difference in ξ between particle pairs increases, resulting in more particles drifting away from the fully burned line. Also the lower values of n limit the number of permutations of particle pairing that are possible.

In addition to the mechanism of mixing, the nature of the reaction zone R in the diffusion flame test affects the performance of the mixing models. The somewhat crude approximation of chemical reaction occurring infinitely fast in a finite area R, with no reaction outside this zone, yields a measure of distortion in the results. Particles whose postmixing value lies just outside R differ greatly in distribution compared to those whose final position is just inside R. The effects of this are seen in the Figs. 3, 6, 10, and 16 at the boundary of the reaction zone. By adoption of a more physically correct reaction zone, with the rate of chemical reaction $S(\xi, Y_P)$ given by a continuous function, infinite at $(\xi_s, 1)$ and decaying to zero at $(\xi, 0)$, these discontinuities in particle position would be reduced.

However, the reaction zone used in the diffusion flame test has the advantage of simplicity, and is satisfactorily in its role as a tool to compare the merits of different mixing models.

Similar joint pdfs to those of Fig. 6 have been obtained by Chen and Kollman [9], using the Modified Curl's model and with the reaction zone proposed by Pope et al. [20]. However, some results of Chen and Kollmann differ significantly from the work presented in this paper. (i.e., Fig. 8 of Chen and Kollmann). Two possible reasons for these differences are as follows.

Firstly, the reaction zone used in the last section of Chen and Kollmann's work consists of an infinitesimally thick region, centered at ξ_s, and extending down to a temperature of 300 K (the equivalent of $Y_P = 0$ in this article). Clearly this zone is not representative of physical reactions, and so results derived from this model can be expected to differ from those described in this paper.

Secondly, Chen and Kollmann's results were obtained for the case of an inhomogeneous flow field, rather than the homogeneous case used in this paper. Previous work [4, 15] has shown that mixing calculations performed by Curl's model and the Modified Curl's model for the case of a passive scalar in an inhomogeneous flow yield a nearly Gaussian distribution of scalar fluctuation, despite non-Gaussian results in homogeneous flow. Therefore it is not unreasonable to suggest that the joint pdf $\mathscr{P}_{\xi Y_P}$ will be affected by the difference in flow field.

6. CONCLUSIONS

It has been shown that Curl's model and the Modified Curl's model incorrectly produce joint pdf's characteristic of distributed combustion when used to model fast or high Da diffusion flames. In addition, the pdf of the mixture fraction $\mathscr{P}_\xi(\zeta)$ is seen to asymptote to a non-Gaussian distribution with infinite flatness μ_4 and superskewness μ_6. In application to inhomogeneous flows though, the pdfs of ξ are closer to Gaussian [4, 15].

A new class of models is presented based on the concept of ordered particle pairing. Two examples of this type of model are described, the

adjacent pairing scheme and the compromise scheme. The adjacent pairing scheme yields excellent results in the diffusion flame test, giving a joint pdf $\mathscr{P}_{\xi Y_P}(\zeta, y)$ that resides very close to the fully burned line $Y_P^f(\zeta)$. However, the pdf of the mixture fraction is seen not to asymptote to the desired Gaussian distribution, but to give a bimodal distribution with flatness and superskewness of 1.5 and 2.9, respectively. The compromise scheme yields a slightly inferior performance in the diffusion flame test compared to the adjacent pairing scheme, with $\mathscr{P}_{\xi Y_P}(\zeta, y)$ showing a greater spread away from $Y_P^f(\zeta)$. The pdf of the mixture fraction however, is seen to adopt a better approximation to a Gaussian with flatness and superskewness of 2.1 and 6.5, respectively. It can be expected that in application to inhomogeneous flows both ordered-pairing schemes will yield pdfs closer to Gaussian than in present tests.

This work was supported in part by the National Science Foundation Grant CBT-8814655. Some computations conducted during the research were performed on the Cornell National Supercomputer Facility, which is supported in part by the National Science Foundation, New York State, the IBM Corporation, and members of the Corporate Research Institute

REFERENCES

1. Pope, S. B., *Prog. Ener. Combust. Sci.* 11:119-192 (1985).
2. Dopazo, C., and O'Brien, E. E., *Acta Astronaut.* 1:1239-1240 (1974).
3. Janicka, J., Kolbe, W., and Kollmann, W., *Proceedings of the 1978 Heat Transfer and Fluid Mechanics Institute*, Stanford CA, Stanford University Press, 1978, pp. 296-312.
4. Nguyen, T. V., and Pope, S. B., *Combust. Sci. Technol.* 42:13-45 (1984).
5. Pope, S. B., and Anand, M. S., *Twentieth Symposium (International) on Combustion*, The Combustion Institute, Pittsburgh, 1986, pp. 403-412.
6. Anand, M. S., and Pope, S. B., *Combust. Flame* 67:127-142 (1987).
7. Pope, S. B., *Eighteenth Symposium (International) on Combustion*, The Combustion Institute, Pittsburgh, 1981, pp. 1001-1010.
8. Pope, S. B., and Correa, S. M., *Twenty-First Symposium (International) on Combustion*, The Combustion Institute, Pittsburgh, 1986, pp. 1341-1348.
9. Chen, J. Y., Kollmann, W., and Dibble, R. W., Sandia Report SAND89-8403, 1989.
10. Curl, R. L. *A.I.Ch.E.J.* 9:175-181 (1963).
11. Pope, S. B., *Combust. Sci. Technol.* 28:131-135 (1982).
12. Janicka, J., Kolbe, W., and Kollmann, W., *J. Nonequil. Thermodyn.* 4:47-56 (1979).
13. Tavoularis, S., and Corrsin, S., *J. Fluid Mech.* 104:311-311 (1981).
14. Eswaran, V., and Pope, S. B., *Phys. Fluids* 31:506-520 (1988).
15. Chen, J. Y., and Kollmann, W. *Seventh Symposium on Turbulent Shear Flows*, Stanford, CA, Stanford University Press, 1989.
16. Masri, A. R., and Pope, S. B., *Combust. Flame* (in press).
17. Masri, A. R., Dibble, R. W., and Bilger, R. W., *Combust. Flame* 71:245-266 (1988).
18. Masri, A. R., Dibble, R. W., and Bilger, R. W., *Combust. Flame* 73:261-285 (1988).
19. Masri, A. R., Dibble, R. W., and Bilger, R. W., *Combust. Flame* 74:267-284 (1988).
20. Pope, S. B., Norris, A. T., and Masri, A. R., Sandia Report SAND89-8220, 1989.
21. Bilger, R. W., in *Turbulent Reacting Flows: Topics in Applied Physics* (P. A. Libby and F. A. Williams, Eds.), Springer-Verlag, Berlin, 1980, Vol. 44, pp. 65-113.
22. Bilger, R. W., *Annu. Rev. Fluid Mech.* 21:101-135 (1989).
23. Peters, N., *Prog. Ener. Combust. Sci.* 10:319-339 (1984).
24. Williams, F. A., *Combustion Theory*, Benjamin/Cummings, Menlo Park, CA, 1985, pp. 373-410.
25. Bilger, R. W., *Twenty-Second Symposium (International) on Combustion*, The Combustion Institute, Pittsburgh, 1988, pp. 475-488.
26. Haworth, D. C., Drake, M. C., and Blint, R. J., *Combust. Sci. Technol.* 60:287-289 (1988).
27. Pope, S. B., *Phys. Fluids* 26:404-407 (1983).
28. David, H. A., *Order Statistics*, 2nd ed., Wiley, New York, 1981.

Received 29, September 1989; revised 14 March 1990

APPENDIX A: MIXING WITHOUT AFFECTING THE MEAN

At time t, the ensemble of N stochastic particles has the ensemble average of the scalar ξ, $\langle\xi\rangle$, given by

$$\langle\xi\rangle(t) = \frac{1}{N}\sum_{i=1}^{N}\xi_i(t). \qquad \text{(A1)}$$

A short time interval δt, later, a group of n particles from the ensemble is given new values of ξ, and the new values of $\langle\xi\rangle$ is

$$\langle\xi\rangle(t+\delta t) = \frac{1}{N}\sum_{i=1}^{N}\xi_i(t+\delta t). \tag{A2}$$

For $\langle\xi\rangle$ not to change with time, we require

$$\langle\xi\rangle(t+\delta t) - \langle\xi\rangle(t) = \frac{1}{N}\sum_{i=1}^{N}\left(\xi_i(t+\delta t) - \xi_i(t)\right) = 0. \tag{A3}$$

As only n particles have been changed due to mixing in the interval δt (see Sec. 4.2), the condition for no change in $\langle\xi\rangle$ can be written as

$$\sum_{i=1}^{n}\left(\xi_{\rho i}^{*} - \xi_{\rho i}\right) = 0, \tag{A4}$$

where $\xi_{\rho i}^{*}$ is the new value of the ith particle and $\xi_{\rho i}$ is the old value.

From Eq. 13 $\xi_{\rho i}^{*}$ can be expressed in terms of $\xi_{\rho i}$ and its partner $\xi_{\rho j}$ (given by the selection matrix S_{ij}). Thus Eq. A4 becomes

$$\sum_{i=1}^{n}\left((1-\alpha)\xi_{\rho i} + \frac{\alpha}{2}\left(\xi_{\rho i} + \sum_{j=1}^{n}S_{ij}\xi_{\rho j}\right) - \xi_{\rho i}\right) = 0, \tag{A5}$$

which can be simplified to

$$\sum_{i=1}^{n}\sum_{j=1}^{n}S_{ij}\xi_{\rho j} = \sum_{i=1}^{n}\xi_{\rho i}. \tag{A6}$$

Since $\xi_{\rho i}$ are random, the above equation is satisfied only if the columns of S_{ij} sum to unity, i.e.,

$$\sum_{i=1}^{n}S_{ij} = 1, \qquad j = 1, 2, \ldots, n. \tag{A7}$$

(A sufficient condition for the satisfaction of Eq. A7 is that $S_{ij} = S_{ji}$, as the event of one particle having two or more partners has been excluded, resulting in the sums of the rows of S_{ij} being equal to unity.) For the expectation of ξ not to change with time, the weaker condition,

$$\sum_{i=1}^{n}P_{ij} = 1, \qquad j = 1, 2, \ldots, n, \tag{A8}$$

is sufficient.

APPENDIX B: GAUSSIAN DECAY OF MIXING MODEL

An approximate analysis is performed to examine the influence of the probability matrix P_{ij} on the shape of the pdf produced by the ordered-pairing model.

In the ordered-pairing model, in the time interval δt (Eq. 12) the mixture fraction of n particles ($\xi_{\rho i}$, $i = 1, 2, \ldots, n$) changes by

$$\xi_{\rho i}(t+\delta t) = \xi_{\rho i}(t) + \frac{\alpha}{2}\left[\xi_{\rho j}(t) - \xi_{\rho i}(t)\right], \tag{B1}$$

where ρ_i and ρ_j are partners, while there is no change in the remaining $(N-n)$ particles. Because α is chosen to be small compared to unity ($\alpha = 0.05$), the discontinuous process given by Eq. 30 can be approximated by the continuous process

$$\frac{\partial\xi}{\partial t} = -\gamma\omega(\xi - \xi^{*}), \tag{B2}$$

where γ is a constant and ξ^{*} denotes the partners mixture fraction.

Let $\mathscr{P}_{\xi}(\zeta;\, t)$ be the pdf of $\xi(t)$. Then from Eq. B2 (by standard methods [1]) we obtain

$$\frac{\partial\mathscr{P}_{\xi}}{\partial t} = -\gamma\omega\frac{\partial}{\partial\zeta}\left[\mathscr{P}_{\xi}\langle\xi^{*} - \zeta \mid \zeta\rangle\right], \tag{B3}$$

where $\langle\xi^{*} \mid \zeta\rangle$ denotes the expectation of ξ^{*} conditioned on $\xi = \zeta$.

We now deduce the form of $\langle\xi^{*} \mid \zeta\rangle$ for the case of $\mathscr{P}_{\xi}(\zeta;\, t)$ decaying as a Gaussian,

$$\mathscr{P}_{\xi}(\zeta;\, t) = \frac{1}{\sqrt{2\pi}\,\sigma_{\xi}}\exp\left(-\frac{\zeta^2}{2\sigma_{\xi}^2}\right), \tag{B4}$$

where $\sigma_{\xi}(t)$ is the standard deviation at time t.

The evolution of this distribution with time is given by

$$\frac{\partial \mathscr{P}_\xi}{\partial t} = \left[\left(\frac{\zeta}{\sigma_\xi}\right)^2 - 1\right]\mathscr{P}_\xi \xi \frac{d \ln \sigma_\xi}{dt}$$

$$= -\frac{\partial}{\partial \zeta}\left(\mathscr{P}_\xi \zeta\right)\frac{d \ln \sigma_\xi}{dt}. \tag{B5}$$

Now $d \ln \sigma_\xi / dt$ is a negative constant, $-\omega$, and so equating Eq. B3 and Eq. B5 yields

$$\gamma\omega\langle \xi^* - \zeta \mid \zeta\rangle = \omega\zeta \tag{B6}$$

or

$$Q(\zeta) \equiv \langle \xi^* \mid \zeta\rangle - \zeta = \zeta/\gamma. \tag{B7}$$

We conclude then, that a mixing model that can be approximated by Eq. B2 yields Gaussian decay if and only if $\langle \xi^* \mid \zeta\rangle$—or equivalently, $Q(\zeta)$—is linearly proportional to ζ.

We now deduce an expression for $\langle \xi^* \mid \zeta\rangle$ given by the ordered-pairing model. Let ξ_i $(i = 1, 2, \ldots, n)$ denote the mixture fraction for the n samples, ordered so that $\xi_1 \leq \xi_2 \leq \cdots \leq \xi_n$. Given the pdf of ξ, $P_\xi(\zeta)$, the probability of a sample $\xi = \zeta$ being the ith order statistic (i.e., $\xi = \xi_i$) is known [28, p. 9]. So also the joint pdf of two order statistics ξ_i and ξ_j is known [28, p. 10], and hence the conditional expectation $\langle \xi_j \mid \xi_i = \zeta\rangle$ can be obtained. In terms of these statistics we have

$$\langle \xi^* \mid \zeta\rangle = \sum_{i=1}^{n}\sum_{j=1}^{n} P_{ij} q_i \langle \xi_j \mid \xi_i = \zeta\rangle. \tag{B8}$$

where P_{ij} is the probability of the ith order particle having the jth order particle as its partner.

The above results are used as follows. For a given pairing scheme (i.e., a given choice of P_{ij}), $Q(\zeta)$ is determined from Eqs. B6 and B7 with the assumption that $P_\xi(\zeta)$ is Gaussian. Plots of $Q(\zeta)$ are shown in Figs. 14 and 15 for the Adjacent-Pairing Scheme and the Compromise-Pairing Scheme, respectively. The closer $Q(\zeta)$ is to a straight line, the more closely the pdf is expected to evolve as a Gaussian.

It is evident that choosing partners that are close in mixture fraction space is incompatible with exactly Gaussian decay. Consider the case of very small ξ_1 (i.e., $\xi_1/\sigma_\xi \ll -1$). For this case $\langle \xi_j \mid \xi_1 = \zeta\rangle$ becomes independent of ζ as ζ tends to $-\infty$. Consequently $Q(\zeta)$ has slope -1 as $\zeta \to -\infty$. And if partners are chosen to be close in mixture fraction space, then $\langle \xi^* \mid \zeta\rangle$ tends to a negative constant $-C$, say, as ζ tends to $-\infty$. Thus as ζ tends to infinity, $Q(\zeta)$ tends asymptotically to the straight line $Q_-(\zeta) = -(C - \zeta)$.

This behavior is evident in figs. 14 and 15. The same considerations for large values of ζ show that $Q(\zeta)$ asymptotes to the straight line $Q_+(\zeta) = C - \zeta$. Clearly, for $C > 0$, there is no straight line that is consistent with both asymptotes.